In vitro models to study imbalanced autophagy under basal conditions and glycation stress, and its implication in skin aging

Maureen Bourtembourg, Caroline Smal, Aline Chrétien, Michel Salmon.

StratiCELL S.A. Crealys Science Park, Rue Sonet 10, B-5032 Isnes, Belgium, tel: +32 81 72 85 82
https://www.straticell.com.

Introduction

Autophagy plays an essential role in cellular homeostasis and stress adaptation through recycling of defective organelles and aberrant proteins, thereby preventing their deleterious accumulation. Whereas its fine-tuned regulation is crucial to ensure the quality control and cytoprotective response, its excessive induction or blockage compromises cell functionality and survival, inducing degenerative changes in human tissues, reminiscent to those associated with aging. Interestingly, such dysfunctional autophagy appears with age but also, to be triggered by advanced glycation end products (AGEs), modified proteins arising from reactions with sugars and reactive carbonyl metabolites such as glyoxal (GO). Accumulated throughout life, AGEs and their precursors alter cellular functions and detoxification systems, leading to premature cellular senescence and, ultimately, the appearance of visible signs of aging. Due to the crosstalk between impaired autophagic potential, glycation stress and accelerated aging, it is of interest to establish *in vitro* standard 2D models to further investigate the regulation of autophagy under challenging conditions mimicking metabolic stress and ageing cells. Besides to offset the lack of such standardized test systems, the use of *in vitro* skin models combining both aging and/or glycation, and autophagy might offer useful tools to assess potential of dermo-cosmetic products against impaired autophagy in pathological and age-related conditions.

Here, we have investigated autophagy regulation on 2D culture models relying on dermal or epidermal components under distinct stress. The first approach consisted in challenging dermal fibroblasts with GO at 0.6 mM for 72h. GO is recognized as an important glycating agent causing accumulation of AGEs and their deleterious damages, as well as fibroblast premature senescence (Sejersen and Rattan, 2007, 2009). The second approach is based on the culture of both young and older keratinocytes. Autophagy was analysed by staining of LC3B (microtubule-associated protein light chain 3), a marker of autophagosome, and analysis of LC3B-II/LC3B-I and p62 (Sequestosome SQTSM1) protein expression by western blot. Treatment with rapamycin and chloroquine (CQ) or bafilomycin A1 were used to activate and block autophagy in order to assess its flux (Klionsky et al., 2008, 2012; Mizushima et al., 2010; Yoshii and Mizushima, 2017).

Preliminary data demonstrated that challenging fibroblasts with GO promoted the accumulation of autophagosomes associated with an impaired degradation of p62, reflecting the cellular responsiveness to metabolic stress as well as autophagy disruption as a manifestation of such glycation stress. GO-based dermal model might allow to further assess the importance of AGEs adducts in the dysregulation of autophagic potential, closely related to aging. In correlation with these data, the propensity of keratinocytes to induce basal autophagy appeared to be altered with age. The comparative study of young and old keratinocytes showed a better autophagic capacity in young keratinocytes than in older ones as measured by autophagic flux. In contrast, when treated with rapamycin, old keratinocytes presented higher levels of autophagy than younger cells, reflecting their better responsiveness to autophagy stimulus and probably an accelerated autophagy process.

Our data support an imbalanced autophagy process with age or in response to metabolic stress known to induce a senescent phenotype. These observations highlight the importance to develop *in vitro* assays as valuable tools to identify promising therapeutic compounds to stimulate autophagy, closely related to extended longevity and delayed skin aging.

Results

GO-mediated alterations of human fibroblasts biology: cell morphology and AGEs production

NHDFs fibroblasts were exposed to 0.6 mM GO and were observed after 72h for morphological changes and cell growth. These culture conditions are reported to induce AGEs formation but also, cellular senescence and the arrest of the cell cycle (Sejersen and Rattan, 2009). The selection of the GO dose was based on a preliminary study consisting in cell treatment with GO at concentration ranging from 0.125 to 2 mM (data not shown).

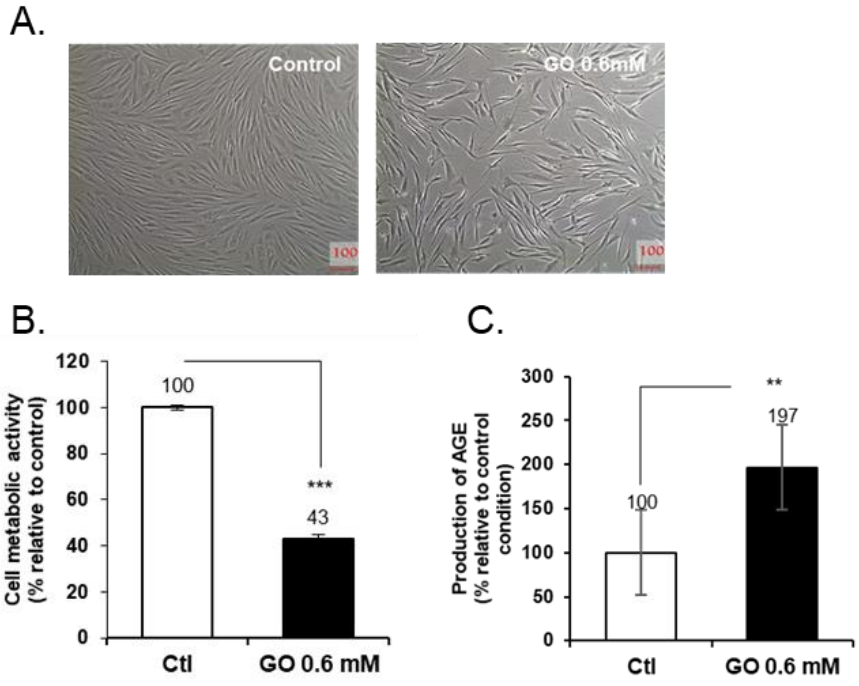

Figure 1. Evaluation of the glyoxal (GO) effect on morphological characteristics and advanced glycation end-products (AGE) formation in NHDFs fibroblasts. *The NHDFs fibroblasts were seeded 24h before changing the medium with Dulbecco's Modified Eagle's Medium (DMEM) supplemented with 1% of foetal bovine serum (FBS). The application of 0.6 mM GO used to mimic an AGE-related cellular stress as in vivo context was performed for 72h after the first 24h of culture in 1% FBS-DMEM.* ***A.*** *The analysis of cell morphology was performed using phase contrast microscopy. The images shown are representative of three independent experiments.* ***B.*** *The metabolic activity, used as an indicator of cell growth was assessed with MTS (3-(4,5-dimethythiazol-2-yl)-5-(3-carboxy-methoxyphenyl)-2-(4-sulfophenyl)-2H-tetrazolium) after 72h of treatment with GO in triplicates of culture (n=3).* ***C.*** *The AGE content was quantified on protein extracts by a specific ELISA assay in triplicates of culture (n=3). Histograms represent the mean of data obtained from the 3 cultures ± Standard Deviation (SD) are reported to the control condition arbitrarily set to 100%. Statistical analysis was performed using bilateral Student's t-test (* 0.01 < P < 0.05; ** 0.001 < P < 0.01; *** P < 0.001) for the comparison of glyoxal to control condition. Abbreviations: Ctl, control; GO, glyoxal; AGE, Advanced Glycation End-products.*

The morphology of NHDFs fibroblasts was first analysed to globally assess the impact of the GO treatment. Cell morphology and appearance in culture dishes allowed to evaluate the cell health and proliferative potential under AGEs-promoting conditions. **Figure 1A** shows that unlike control condition, cells exposed to GO for 72h became enlarged, flattened and irregularly shaped, which are notably characteristic of senescent cell phenotype, as depicted in the literature (Cristofalo et al., 2004; Sejersen and Rattan, 2009). Interestingly, it was also noticed that these GO-challenged cells exhibited a poor cell growth. This was confirmed by the cell growth assay. At 72h of treatment, the signal of metabolic activity (< 50% relative to the control) which reflects the cell proliferation rate, is significantly decreased in comparison to control cells (**Figure 1B**), supporting the GO-mediated cell growth arrest and the appearance of a phenotype similar to senescent cells (Sejersen and Rattan, 2009). To verify the efficiency of GO treatment to reproduce an *in vitro* AGEs-enriched environment, the intracellular content in AGEs was quantified by ELISA assay in NHDFs fibroblasts. The results obtained are illustrated in the **Figure 1C** and indicated that GO treatment for 72h significantly increased AGEs production and accumulation, reflecting the property of this reactive dicarbonyl compound to stimulate the glycation of proteins.

Therefore, as GO induced alterations which are reminiscent to the typical appearance of senescent fibroblasts, and increased AGEs formation, the data support that cell exposure to 0.6 mM GO for 72h is a relevant model to mimic senescence and glycation stress and, to investigate autophagy.

GO-mediated impairment of autophagy: increase of the autophagosome size and number, disruption of degradation capacities and flux

Previous studies have shown a link between methylglyoxal (MGO), an important precursor of intracellular AGEs, and autophagy dysregulation in the context of diabetic and degenerative conditions (Chang et al., 2015; Dafre et al., 2017; Fang et al., 2015; Liu et al., 2012). However, the specific regulation of autophagy in dermal cells under challenging conditions with a reactive glucose metabolite, has not yet been characterized.

In line with the previous observations, GO may have a role in the autophagy modulation in skin aging. To investigate such a role, fibroblasts monolayers were treated with 0.6 mM GO for 72h, with or without 3 µM chloroquine (CQ), a lysosomal protease inhibitor which blocks the dynamic process of autophagy and, prevents the degradation of autophagosomes and their specific contents in lysosome. This treatment is expected to be optimal for monitoring the autophagy flux, widely used as a relevant indicator of autophagy activity (Jiang and Mizushima, 2015; Mizushima et al., 2010; Pugsley, 2017; Yoshii and Mizushima, 2017).

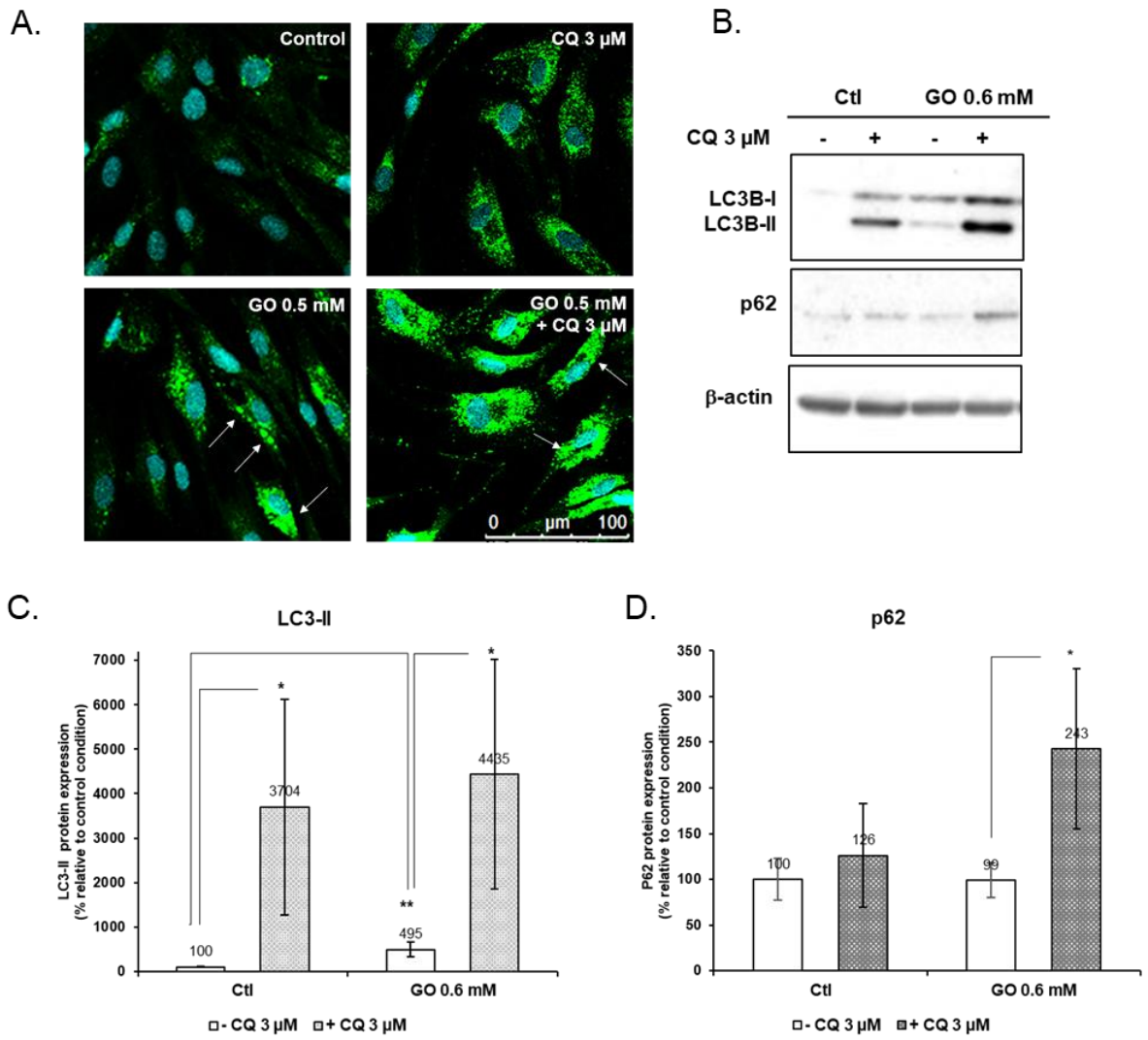

Figure 2. Evaluation of the glyoxal (GO) effect on the regulation of autophagy pathway through the analysis of two autophagic markers, LC3B and p62, and their turnover in NHDFs fibroblasts. *The NHDFs fibroblasts were seeded 24h before changing the medium with Dulbecco's Modified Eagle's Medium (DMEM) supplemented with 1% of foetal bovine serum (FBS). After these first 24h, the application of 0.6 mM GO (or 0.5 mM for culture on glass slides) used to mimic an AGE-related cellular stress as in vivo context was performed for 72h in presence, or not, of 3µM chloroquine (CQ) used to inhibit the autophagy flux and avoid the degradation of autophagic structures and cargoes.* ***A****. Immunostaining of LC3B in NHDFs fibroblasts indicated the number of LC3B-positive punctae and their localization. Cells were fixed with ice-cold methanol and incubated with rabbit polyclonal anti-LC3B primary antibody and then with Alexa 488-labeled goat anti-rabbit Fab secondary antibody. Cells were examined by confocal microscopy and pictures are taken for each condition (n=3 pictures/culture and n=9 pictures/condition). Magnification 40x.* ***B.*** *Western blot analysis of LC3B-II/LC3B-I and p62 was performed from 3 µg of each protein extract. B-actin expression is shown as a loading control. Cultures were performed in triplicates (n=3).* ***C., D****. LC3B-II and p62 bands were quantified using ImageJ software. Following 72h of treatment with glyoxal under low serum culture conditions, the analysis of cell morphology (A), metabolic activity (B) and AGE content (C) was performed from triplicates of culture (n=3). Histograms represent the mean of data obtained from the 3 cultures ± Standard Deviation (SD) are reported to the control condition arbitrarily set to 100%. Data are normalized to the optical density of b-actin bands, used as loading control. Statistical analysis was performed using unilateral Student's t-test (* 0.01 < P < 0.05; ** 0.001 < P < 0.01; *** P < 0.001) for the comparison of glyoxal to control condition. Abbreviations: Ctl, control; GO, glyoxal; CQ, chloroquine.*

The regulation of autophagy by glycated adducts was first examined by immunofluorescence and confocal microscopy to visualize the labelled LC3B-positive puncta, corresponding to the formation of autophagosomes. As observed on the **Figure 2A**, the number and, the size of LC3B dots appeared greater in dermal fibroblasts when exposed to GO compared with those in cells cultured under basal conditions. The concomitant treatment with CQ appeared to increase the GO effect by stabilizing the generated autophagosomes and avoiding their rapid cellular degradation (**Figure 2A**), indicating that glyoxal treatment promoted autophagosome accumulation. Interestingly, in GO-treated cells, the acquisition of dots with a superior size and their accumulation was more marked in some cells than others, reflecting a distinct cell responsiveness to treatment. However, the addition of CQ abolished this non-homogenous LC3B staining, indicative of the potentiation of GO to activate each cell but, according probably a specific cell responsiveness. To note, the intensity of LC3B staining seemed to be amplified when cells were exposed to GO and CQ, compared to CQ only, supporting further a glyoxal-mediated autophagosome formation.

Since the conversion of the cytosolic form of LC3 protein (LC3-I) to its membrane-bound by the addition of phosphatidylethanolamine (PE) (LC3-II) is required for the formation of autophagosomes, a western blot analysis was performed in order to discriminate both forms and focus specifically on the protein expression of LC3-II which reflects the number of autophagosomes present at the specific time point of the analysis (**Figure 2B-C**).

In correlation with the previous observations on the confocal imaging, the basal level of LC3B-II protein was significantly higher (5 fold) in GO-treated cells compared to control, supporting the increase in number of autophagosomes under glycation stress. As the increased appearance of autophagosomes and protein level LC3-II can reflect the induction of autophagy and/or inhibition of autophagosome clearance, the autophagy activity was analysed by determining the levels of LC3-II in presence or in absence of CQ (autophagy flux) (**Figure 2B-C**). As expected, the presence of CQ induced significantly the accumulation of LC3B-II proteins compared to LC3B-II protein levels in CQ-negative samples, reflecting the efficient autophagy blockage and inhibition of autophagosome degradation. However, the difference in protein abundance between samples with and without CQ was found similar in cells exposed, or not, to GO. This absence of significant induction of autophagy flux which was accompanied by increased amount of LC3B-II suggested that GO impairs the autophagy process, with a suppression of effective substrate degradation, leading to autophagosome accumulation.

To further test this hypothesis and as complementary analysis to LC3B turnover assay, levels of the autophagy substrate p62 were examined by western blot, as shown on **Figure 2B-D**. The autophagy marker p62 (SQSTM1) mediates the delivery of ubiquitinated proteins to autophagosomes through its ability to interact with LC3, resulting in their efficient degradation by autophagy. As p62 itself undergoes autophagic degradation, the cellular expression levels of p62 inversely correlate with autophagy activity (Mizushima et al., 2010).

Contrary to what was observed for LC3B-II protein levels, no significant change in the protein abundance of p62 was observed in cells cultured with or without GO, likely to reflect the unstimulated p62 degradation and, therefore, suggesting a basal autophagy activity in GO-treated cells. However, such as LC3B-II, western blot analysis of p62 represents only a snapshot of a dynamic process. Therefore, measurement of p62 in the presence or absence of lysosomal blockade with CQ can provide further insights about the rate of transit of autophagosome cargo through lysosomal degradation (autophagic flux). Interestingly, the addition of the flux inhibitor CQ increased significantly the level of

p62 protein in cells when cultured with GO. Although slightly enhanced, such effect on p62 protein abundance was not observed in cells cultured in absence of GO.

Taken these data into consideration, by inhibition of the autophagic degradation, CQ allows to accumulate p62 protein within GO-treated cells at a more pronounced level than those observed in basal conditions, suggesting that the combined treatment GO may have a synergistic effect with CQ, thus accumulating p62. This effect was accompanied by the absence of apparent modification of p62 amounts when cells are cultured without CQ, supporting further that the combination of GO/CQ improves the transcriptional regulation of p62 than its degradation. Therefore, it would worth to perform complementary analyses, such as evaluate the gene expression levels of the autophagy marker and its protein abundance along earlier timing, in order to inform about the competence of fibroblasts for the autophagy stimulation under glycation stress. This could be beneficial to enhance the understanding of autophagy dysregulation in context of senescence and AGEs, toxic molecules known to promote skin aging and the development of numerous degenerative disorders.

Altogether, this first model provides evidence to demonstrate that GO, a glycolysis metabolite and precursor of AGEs impairs the autophagy pathway in human skin fibroblasts cultures. Such effect may operate through the autophagy dysregulation, resulting in the decreased autolysosomal degradation of autophagosomes (LC3B-bound vacuoles) and specific cargo. As a consequence to these alterations, proteostasis and an efficient removal of damaged organelles might be dysfunctional within cells, leading progressively to protein aggregate burden, hallmark of aging. Therefore, the use of GO challenge on NHDFs fibroblasts to induce autophagy deficit as a standardized model might constitute an original alternative to the culture of old dermal cells. By its association of both glycation and senescence, the GO model represents a promising tool to test the potential of compounds to restore or improve beneficial autophagy, preventing the appearance of cell aging signs and preserving the cell health capital.

Given the crucial role of autophagy dysregulation in aging, disruption of its degradative capacities by glycated adducts paves the way to further investigations on the related mechanisms. Deeper analyses of this model are ongoing in order to better characterize this model.

Comparison of autophagic capacity in young and old NHEKs keratinocytes: autophagy basal level is altered during aging but old NHEKs present a better responsiveness to autophagy stimulus

NHEKs isolated from young and old donors were cultured during 18h with rapamycin (10 µM) used to stimulate the autophagy process or DMSO at 0.1% corresponding to rapamycin's solvent. The treatments were performed in presence or absence of bafilomycin A1 (200 nM) used as lysosomotropic agent to block LC3-II degradation and so, to allow autophagic flux measurement. After treatments, proteins were extracted and the levels of LC3B were assessed by western blot analysis, as shown in **Figure 3A**. LC3B-II/β-actin protein ratios are presented in **Figure 3B**. The autophagic flux calculated from LC3B-II levels in presence or absence of bafilomycin A1 is presented as well (**Figure 3C**).

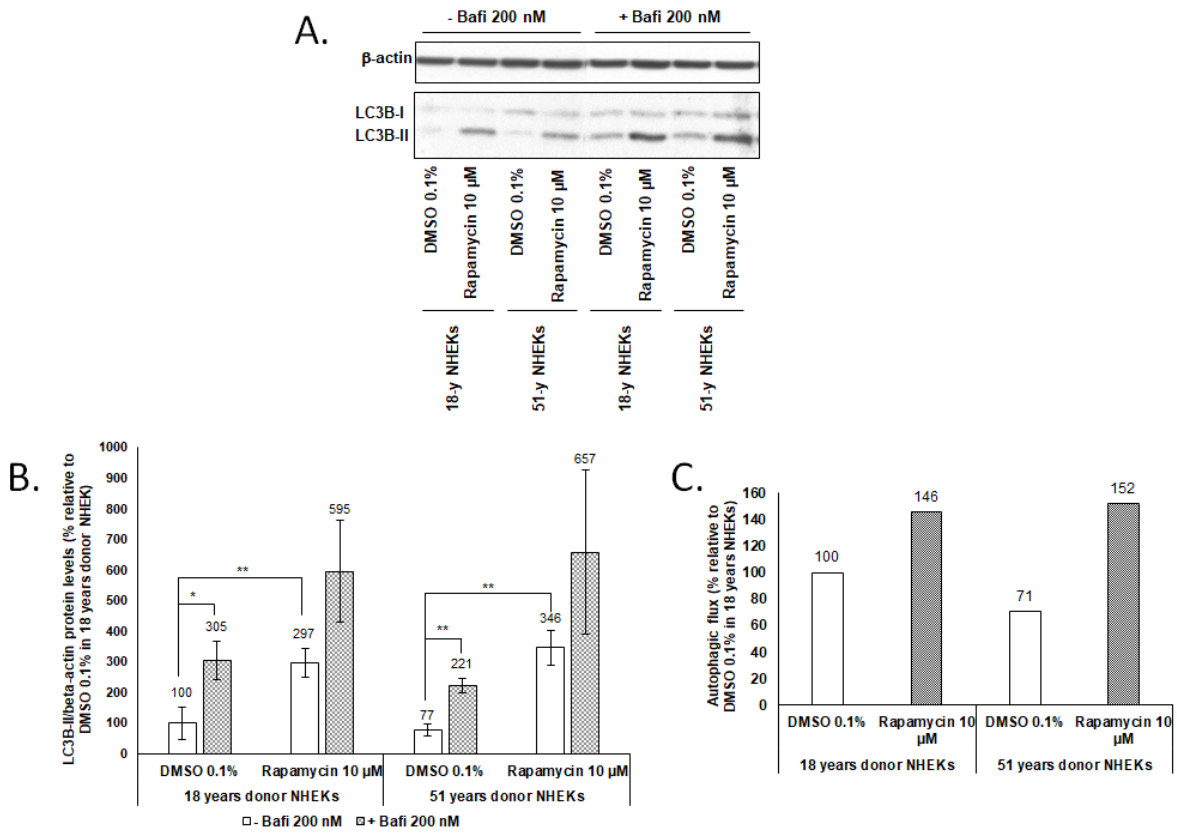

Figure 3. Evaluation of the age effect on the regulation of autophagy through LC3B analysis, in young and old NHEKs keratinocytes. *The 18 years and 51 years NHEKs keratinocytes were seeded 24h before the treatment with the reference molecules. Cells were treated with rapamycin at 10 µM or DMSO 0.1% (corresponding to rapamycin's solvent) in absence or presence of bafilomycin A1 at 200 nM used as lysosomotropic agent to stop the degradation of LC3B-II. Following 18h of treatment, proteins were extracted from triplicates of culture (n=3).* ***A.*** *LC3B western blot analysis was performed from 6 µg of each protein extracts. Beta-actin expression is shown as a loading control.* ***B.*** *LC3B-II bands quantification was done using ImageJ software. Histograms represent the mean of LC3B-II/β-actin expression data obtained from the 3 cultures ± Standard Deviation (SD). Data are reported to the DMSO 0.1% condition in 18-years NHEKs arbitrarily set to 100%. Statistical analysis was performed using bilateral Student's t-test (* 0.01 < P < 0.05; ** 0.001 < P < 0.01) for the comparisons to respective control conditions.* ***C.*** *Autophagic flux was calculated from expression data. Autophagic flux is expressed in % relative to the DMSO 0.1% condition in 18-years NHEKs arbitrarily set at 100%.*

The basal levels of LC3B-II, reflecting the autophagosomes number, were compared between young and old NHEKs. The autophagic flux was quantified as well. The autophagic flux, measured as LC3 turnover, is a more reliable indicator of autophagic activity than measurements of the autophagosome numbers. It represents the amount of LC3 that is delivered to lysosomes for degradation, calculated by doing the difference in the amount of LC3-II detected in presence and absence of lysosomal inhibitors (He and Klionsky, 2009; Klionsky et al., 2008, 2012; Mizushima and Yoshimori, 2007; Mizushima et al., 2010).

Our data showed that old NHEKs present a decreased (but not significant) LC3B-II level and an impaired autophagic flux as compared to younger NHEKs.

A decrease in the autophagic activity has already been convincingly demonstrated in aging models (Martinez-Vicente et al., 2005). It has been proposed that accumulation of aberrant or functionally disabled mitochondria and other damaged structures observed during the aging process is a consequence of an age-related decline in autophagic and lysosomal activity (Demirovic et al., 2015; Gelino and Hansen, 2012; Martinez-Vicente et al., 2005; Rajawat and Bossis, 2008).

It appeared as well that treatment with rapamycin (10 µM) during 18h increased the autophagic flux of both young and old NHEKs keratinocytes. This has been duly documented for a variety of cell types and organisms (Kim and Guan, 2015). Nevertheless, the increase of the autophagic flux is more important in older keratinocytes reflecting a better responsiveness to autophagy stimulus.

Taken these observation into consideration, NHEKs keratinocytes from older donors present a lower basal autophagy level but a better responsiveness to autophagy stimulus. It is therefore likely that they would be the best option to maximize the chance to identify compounds or extracts to increase the autophagy capacity in epidermal cells.

Treatment of young and old keratinocytes with GO should be considered as an important subject for future studies and might constitute a useful cellular model for aging research. As protein aggregation and reduced detoxification system capacity represent hallmarks of aging, the use of such stressor on keratinocytes might reveal new insights about the autophagy role in progression of aging and deleterious outcomes. The combination of both models could add a plus value to the present interpretations.

Materials and methods

Cell culture

NHDFs fibroblasts model:

Normal Human foreskin-derived Dermal Fibroblasts (NHDFs; ATCC, CRL-2522) were grown in Dulbecco's Modified Eagle Medium (DMEM, Gibco/Life Technologies, 31885) supplemented with 10% of Foetal Bovine Serum (FBS, Gibco/Life Technologies, 10270) and antibiotics (penicillin/streptomycin, Gibco/Life Technologies, 15140). The cells were maintained in a humidified incubator at 37°C with a 5% CO2 atmosphere. At 24h after seeding, cells cultured in DMEM containing 10% of FBS were transferred to DMEM in the presence of 1% of FBS to allow to exert a better control of the amount of glycated products, as serum proteins are frequent targets of modifications by reactive carbonyl compounds such as GO (Nowotny, Jung, Hohn, Weber, & Grune, 2015).

Young and old NHEKs keratinocytes models:

Normal Human Epidermal Keratinocytes isolated from biopsies of an 18 years donor and a 51 years donor were grown in Epilife Medium (Gibco/Life Technologies, M-EPI-500-A) supplemented with Human Keratinocytes Growth Supplement (HKGS, Gibco/Life Technologies, S-001-5) and gentamycin (Gibco/Life Technologies, 15710-049). The cells were maintained in a humidified incubator at 37°C with a 5% CO2 atmosphere.

Cell treatment

NHDFs fibroblasts treatment:

NHDFs cells were treated with glyoxal (GO; Sigma 50649) used at 0.6 mM for 72h in order to reproduce senescent profile and an *in vitro* AGEs-enriched environment with their related cellular damages. Due to the greater cell sensitivity to challenging conditions when they are cultured on glass slides system, the GO concentration has been adapted to 0.5 mM. The GO treatment was combined, or not, with 3 µM chloroquine (CQ; Sigma, C6668) used as a autophagy inhibitor that impairs lysosomal acidification and consequently, prevent the fusion of autophagosomes with lysosomes and block autophagy flux. The treatments were performed in triplicate (n=3).

NHEKs keratinocytes treatment:

NHEKs cells from the two donors (18 years and 51 years) were treated for 18h with 10 µM rapamycin (Sigma, 37094) in order to induce autophagy process. DMSO at 0.1% (corresponding to rapamycin's solvent) was used as control condition. This treatment was combined, or not, with bafilomycin A1 (Sigma, B1793) at 200 nM, used as lysosomotropic agent to inhibit the fusion of autophagosomes with lysosomes, resulting in the blockage of autophagic flux and the increase of LC3-II levels in NHEKs keratinocytes. The treatments were performed in triplicate (n=3).

Measurement of metabolic activity

A measurement of metabolic activity was performed by using the MTS reagent (3-(4,5-dimethythiazol-2-yl)-5-(3-carboxy-methoxyphenyl)-2-(4-sulfophenyl)-2H-tetrazolium) (Promega, G3581) after the treatment with GO. The metabolically active cells convert the MTS tetrazolium compound into a colored formazan product that is soluble in cell culture medium. The optical density of produced

formazan measured at 490 nm by spectrophotometry (*Biochrom Asys UVM 340 Microplate Reader)* is directly proportional to the number of viable cells.

Measurement of AGEs content

To detect and quantify the level of AGEs formation, the protein extracts were collected and stored at -80°C. Total protein concentration was determined by Bradford colorimetric assay (Thermo Fisher Scientific, 23200) and measured at 450 nm by spectrophotometry (*Biochrom Asys UVM 340 Microplate Reader)*. Global AGEs levels were analysed by using ELISA kits (Cell Biolabs, STA-817), according to the supplier's instructions. The obtained values were normalized to the protein concentrations.

LC3B immunostaining and confocal microscopy

NHDFs fibroblasts were fixed with ice-cold methanol for 5 min, rinsed with PBS and stored at 4°C until the immunostaining assay. Cells were incubated in a blocking solution (PBS- 0.1 %Tween 20 - 0.3 M Glycine - 1% BSA – 10% Normal Goat serum) for 1h at RT. Then, cells were incubated with the anti-LC3B antibody (Cell Signalling, 2775) used at 1/200 overnight at 4°C. Next day, cells were incubated with the specific anti-rabbit antibody, conjugated to a fluorescent dye (Alexa Fluor 488; Invitrogen, A11008) used at 1/250 for 1h at RT. Nuclei were stained with DAPI (4',6'-diamidino-2-phénylindole; Thermo Fisher, D1306). After each incubation step, cells were washed with PBS – 0.1% Tween 20. Slides were mounted with Mowiol and observed with a confocal microscope (TCS Leica,lens 40x). Images were processed with the Leica LAS AF lite software.

LC3B-II and p62 immunoblot analysis

After treatments, proteins were extracted and quantified by spectrophotometric measurement (Bradford assay; 660 nm: Thermo Scientific, 23200) and stocked at -80°C until further use in western blot. For all the conditions, the same quantity of protein extracts was loaded on polyacrylamide SDS-PAGE gel (NuPAGE Novex 12% Bis-Tris; Invitrogen NP0342BOX) and was separated by electrophoresis using the *mini gel tank and blot module set* (Invitrogen, NW2000) following an optimized protocol (1h30 at 125V for LC3B and p62). Proteins were then transferred on polyvinylidene fluoride (PVDF) membranes by the use of the transfer device provided with the mini gel tank (1h at 20V). The membranes were then placed in presence of an antibody directed against the interest protein, LC3B (Cell Signalling, 2775) or p62 (Cell Signalling, 5114), and then in presence of the secondary antibody (anti-rabbit coupled to peroxidase; GE Healthcare-Amersham, NA934). For normalization purpose, membranes were then put in presence of an antibody directed against the ubiquitous protein β-actin (Cell Signalling; 3700) followed by the secondary antibody (anti-mouse coupled to peroxidase; GE Healthcare-Amersham, NA931VS).The plots were visualized on films (GE Healthcare-Amersham hyperfilms, 28-9068-36) by auto-radiography after incubation of membranes with a chemiluminescent substrate of the peroxidase (ECL substrate; GE Healthcare-Amersham, RPN2135). For each sample, data were normalized by reporting the intensity of the plot obtained for LC3B-II or p62 protein to the intensity of the plot obtained for β-actin.

Statistical analysis

Data are presented as means ± Standard Deviation (SD) as indicated in the figures. Analysis of data was performed by a t test for the comparison of treated conditions versus untreated control or positive control. Statistical significance of differences was evaluated by Student's t test (*: $0.01<P<0.05$; **: $0.001<P<0.01$; ***$P < 0.001$).

References

Chang, Y.-C., Hsieh, M.-C., Wu, H.-J., Wu, W.-C., and Kao, Y.-H. (2015). Methylglyoxal, a reactive glucose metabolite, enhances autophagy flux and suppresses proliferation of human retinal pigment epithelial ARPE-19 cells. Toxicol. Vitro Int. J. Publ. Assoc. BIBRA *29*, 1358–1368.

Cristofalo, V.J., Lorenzini, A., Allen, R.G., Torres, C., and Tresini, M. (2004). Replicative senescence: a critical review. Mech. Ageing Dev. *125*, 827–848.

Dafre, A.L., Schmitz, A.E., and Maher, P. (2017). Methylglyoxal-induced AMPK activation leads to autophagic degradation of thioredoxin 1 and glyoxalase 2 in HT22 nerve cells. Free Radic. Biol. Med. *108*, 270–279.

Demirovic, D., Nizard, C., and Rattan, S.I.S. (2015). Basal level of autophagy is increased in aging human skin fibroblasts in vitro, but not in old skin. PloS One *10*, e0126546.

Fang, L., Li, X., Zhong, Y., Yu, J., Yu, L., Dai, H., and Yan, M. (2015). Autophagy protects human brain microvascular endothelial cells against methylglyoxal-induced injuries, reproducible in a cerebral ischemic model in diabetic rats. J. Neurochem. *135*, 431–440.

Gelino, S., and Hansen, M. (2012). Autophagy - An Emerging Anti-Aging Mechanism. J. Clin. Exp. Pathol. *Suppl 4*.

He, C., and Klionsky, D.J. (2009). Regulation Mechanisms and Signaling Pathways of Autophagy. Annu. Rev. Genet. *43*, 67–93.

Jiang, P., and Mizushima, N. (2015). LC3- and p62-based biochemical methods for the analysis of autophagy progression in mammalian cells. Methods San Diego Calif *75*, 13–18.

Kim, Y.C., and Guan, K.-L. (2015). mTOR: a pharmacologic target for autophagy regulation. J. Clin. Invest. *125*, 25–32.

Klionsky, D.J., Abeliovich, H., Agostinis, P., Agrawal, D.K., Aliev, G., Askew, D.S., Baba, M., Baehrecke, E.H., Bahr, B.A., Ballabio, A., et al. (2008). Guidelines for the use and interpretation of assays for monitoring autophagy in higher eukaryotes. Autophagy *4*, 151–175.

Klionsky, D.J., Abdalla, F.C., Abeliovich, H., Abraham, R.T., Acevedo-Arozena, A., Adeli, K., Agholme, L., Agnello, M., Agostinis, P., Aguirre-Ghiso, J.A., et al. (2012). Guidelines for the use and interpretation of assays for monitoring autophagy. Autophagy *8*, 445–544.

Liu, H., Yu, S., Zhang, H., and Xu, J. (2012). Angiogenesis impairment in diabetes: role of methylglyoxal-induced receptor for advanced glycation endproducts, autophagy and vascular endothelial growth factor receptor 2. PloS One *7*, e46720.

Martinez-Vicente, M., Sovak, G., and Cuervo, A.M. (2005). Protein degradation and aging. Exp. Gerontol. *40*, 622–633.

Mizushima, N., and Yoshimori, T. (2007). How to Interpret LC3 Immunoblotting. Autophagy *3*, 542–545.

Mizushima, N., Yoshimorim, T., and Levine, B. (2010). Methods in Mammalian Autophagy Research. Cell *140*, 313–326.

Pugsley, H.R. (2017). Quantifying autophagy: Measuring LC3 puncta and autolysosome formation in cells using multispectral imaging flow cytometry. Methods *112*, 147–156.

Rajawat, Y.S., and Bossis, I. (2008). Autophagy in aging and in neurodegenerative disorders. Horm. Athens Greece *7*, 46–61.

Sejersen, H., and Rattan, S.I.S. (2007). Glyoxal-induced premature senescence in human fibroblasts. Ann. N. Y. Acad. Sci. *1100*, 518–523.

Sejersen, H., and Rattan, S.I.S. (2009). Dicarbonyl-induced accelerated aging in vitro in human skin fibroblasts. Biogerontology *10*, 203–211.

Yoshii, S.R., and Mizushima, N. (2017). Monitoring and Measuring Autophagy. Int. J. Mol. Sci. *18*.